Site-Specific Biomimetic Precision Chemistry of Bimodal Contrast Agent with Modular Peptides for Tumor-Targeted Imaging

Bingbo Zhang,[†] Jun Wang,[†] Jiani Yu,[†] Xiangming Fang,*[‡] Xiuli Wang,[†] and Donglu Shi*[§,⊥]

[†]Institute of Photomedicine, Shanghai Skin Disease Hospital; The Institute for Biomedical Engineering & Nano Science, Tongji University School of Medicine, Shanghai 200443, China

[‡]Department of Radiology, Wuxi People's Hospital, Nanjing Medical University, Wuxi 214023, China

[§]The Institute for Translational Nanomedicine, Shanghai East Hospital; The Institute for Biomedical Engineering & Nano Science, Tongji University School of Medicine, Shanghai 200092, P. R. China

[⊥]The Materials Science and Engineering Program, Department of Mechanical and Materials Engineering, College of Engineering and Applied Science, University of Cincinnati, Cincinnati, Ohio 45221, United States

Ⓢ *Supporting Information*

ABSTRACT: Various biomimetic nanoparticles have been fabricated for cancer nano-theranostics with a diverse range of proteins. However, the operating mechanisms of these reactions are still unclear, especially on the interaction between metal ions and protein, the precise binding sites, and the existence format of nanoparticles. Assuming the shortening of the amino acids sequence into several, namely short peptides, it would be much easier to investigate the biomimetic reaction mechanism. In this study, a modular peptide, possessing Au^{3+} ion coordination motifs and a Gd^{3+} ion chelation sequence, is designed and synthesized. This peptide is experimentally found effective in site-specific biomimetic synthesis of paramagnetic fluorescent gold nanoclusters (pAuNCs) with a quantum yield of 6.8%, deep red emission at 676 nm, and potent relaxivity. The gel electrophoresis result declares that the two imaging motifs in pAuNCs are quite stable. In vivo fluorescence−magnetic resonance bimodal imaging show significant tumor enhancement by pAuNCs in tumor-bearing mice. In vivo biodistribution and toxicity studies reveal that pAuNCs can be gradually cleared from the body without damage. This study presents a modular peptide that can incubate multifunctional nanoparticles in a biomimetic fashion and hopefully provides a strategy for the investigation of the mechanism of protein-mediated biomimetic synthesis.
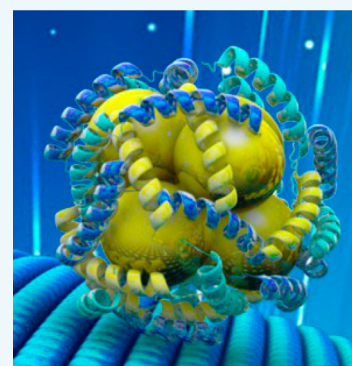
Although the burgeoning advancement in cancer nano-theranostics has much to offer for improving diagnostics and medical treatments,[1−4] new strategies in this field need to be further developed in terms of rational design of intelligent imaging and theranostic probes, particularly in a green and facile fashion. In the past decade, the rapid advancement of nanotechnology has enabled the emergence of various approaches for the fabrication of functional nanostructured materials for cancer imaging and therapy. These synthetic methods, including co-precipitation,[5] sol−gel,[6] hydrothermal synthesis,[7] microemulsion,[8] thermal decomposition,[9] etc., have been well-developed along with the associated synthetic theories. In the construction of the multifunctional nanostructures, in the overwhelming majority of cases, functional units are assembled upon certain nanoparticle scaffold−architecture step-by-step. Quite often, these final constructs are achieved with versatile capabilities[10,11] (for instance, the combined fluorescent imaging and magnetic resonance imaging (MRI)). However, these methods and nanostructures encounter disadvantages including tedious synthetic processing, harsh reaction conditions, toxicity concerns, and environmentally unfriendly metrics, which are particularly not suitable for biomedical applications.[12−14] Furthermore, the assembled nanosystems, even though afforded with multifunction, are taking the risks of enlarged sizes, structural instability, adverse reactions with each other, and reduced surface space utilization. Thus, there remains a strong need for advanced multifunctional nanostructure designs and synthetic strategies that can demonstrate: (1) robustly facile fashion without requiring complex assembling or conjugation chemistries; (2) site-specific precision synthesis, embodying each function moiety in its intended position without interference; and (3) green chemistry without involvement of organic solvents, heating, or refluxing.

Biomimetic chemistry has been recently developed that can cumulatively contribute important elements for achieving the above goals.[15] We have previously shown that bovine serum albumin (BSA) protein can be used efficiently for the phase transfer of hydrophobic quantum dots into aqueous phase by metal affinity coordination and hydrophobic interaction with the quantum dot surfaces in the condition of ultrasound.[16] This

technique has been extended onto other nanoparticles (NPs), such as Cd-free quantum dots,[17] iron oxide NPs,[18] and up-conversion NPs.[19] Furthermore, BSA was found talented in the direct biosynthesis of fluorescent gold nanoclusters in a facile fashion.[20,21] We have also developed Gd-based NPs for MR angiography with BSA via a biomimetic synthesis. By this approach, the Gd−CuS NPs were synthesized as a theranostic agent for in vivo photoacoustic−magnetic resonance (MR) imaging-guided tumor-targeted photothermal therapy.[22] The synthesis chemistry relied mostly on a series of chemoselective amino acid triggered chemical events, including ion chelation, crystal nucleus formation, and further growth.[21] However, in an initial stage, various biomimetic NPs have been fabricated via this robust strategy for cancer nanotheranostics with a diverse range of proteins.[15,23] However, the operating mechanisms of these reactions are still unclear, especially on the interaction between metal ions and protein, the precise binding sites, and the existence format of NPs.

Proteins are known as large biomolecules, or macro-molecules, consisting of one or more long chains of amino acid residues. As such, it causes the complexity in biomimetic chemistry. Through current literatures, it can be found that most of proteins, particularly for gold NPs biosynthesis, contain cysteine (C), tyrosine (Y), and tryptophan (W).[15,23] Assuming shortening of the amino acids sequence into several, namely short peptides, it would be much easier to identify the biomimetic reaction mechanism. Based on this hypothesis and structural similarity between protein and peptide, we herein design a unique structure of short peptide of cyclic (Pro−Asp−Trp−Glu−Gly−Pro−Glu−Arg−Asp−Lys (Cys−Cys−Tyr−C6)) (termed CCY−C6−CP) with a molecular weight of 1692.9 (Scheme 1). The matrix-assisted laser desorption−ionization time-of-flight mass spectrometry (MALDI-TOF MS) of pure CCY−C6−CP peptide is presented in Figure S1. As shown in Scheme 1, this peptide displays three internal functional modules or domains. Domain I of the Cys−Cys−Tyr (CCY) motif can capture Au^{3+} ions by the −SH groups of cysteine and further in situ site-specifically reduce them into gold nanoclusters by the phenolic group of tyrosine. Domain II of cyclic peptide (CP) with multiple carboxyl sequences is customized for Gd^{3+} chelation. The design idea of cyclic peptide for Gd^{3+} chelation comes from a small molecule structure of 1,4,7,10-tetraazacyclododecane-1,4,7,10-tetraacetic acid (DOTA). The molecule consists of a central 12-membered tetraaza (i.e., containing four nitrogen atoms) ring. DOTA is used as a complexing agent, especially for lanthanide ions for medical MRI. Domain III of C6 is arranged as a flexible spacer linker. This modular peptide with separated functional domains is specially designed and attempted for in situ site-specific biomimetic synthesis of multifunctional nanoarchitecture in a precision chemistry fashion.

In a typical synthesis, Au^{3+} ions were added into the solution of peptide at 37 °C, whereupon Au^{3+} ions can be captured by the thiol groups of domain I to form bidentate Au thiolates intermediates.[24] After stirring for 3 min for thorough mixing, the pH value of solution was adjusted to ca. 10.5 with 2.0 N NaOH, provided alkaline environment to initiate reduction of Au^{3+} ions to Au NPs via the phenolic group of tyrosine in domain-I. The detailed reaction mechanism was discussed in literatures.[24,25] The resulting bright yellow solution shows a broad absorption band ranging from 250 to nearly 600 nm (Figure S2), in which the absorption peak at 275 nm is the characteristic absorption of tyrosine at pH ≈ 7. The peak at 275 nm is presented on the peptide (black) and pAuNCs (red) in neutral environment. This peak has a slight red shift in the alkalized CCY−C6−CP solution (blue).[26,27] Interestingly, the fluorescence intensities of the resulting samples are found to be highly dependent on the amount of NaOH added and the Au^{3+}-to-peptide ratio. Parallel experimental investigation on the reaction parameters shows that, for a certain amount of peptide, either overly excessive or diluted Au^{3+} ions or NaOH is unfavorable to fluorescence emission (Figures S3 and S4). It suggests that the optimum feeding molar ratio of Au^{3+}/peptide/NaOH be 1:0.944:15.2. The resultant AuNCs shows an intense red emission at peak of 676 nm (Figure 1A). Compared with rhodamine 6G, the quantum yield of the optimized AuNCs is found as ca. 6.8%, which is similar to that of the protein-mediated gold nanoclusters.[21] In the protein-mediated biosynthesis of gold nanoclusters, the emission peak is mainly located at a range from 640 to around 690 nm.[23] The peak emission at 676 nm in this study is also located in this range.

AuNC core size and distribution were measured by high-resolution TEM (Figure 1B). The mean size of AuNCs is 1.25 ± 0.2 nm (Figure S5). This size is consistent with other findings that fluorescent AuNCs are confined with a very small core size, exhibiting a strong quantum confinement effect.[21] In this study, the size of pAuNCs was found difficult to tune. However, the fluorescent intensity can be controlled by the feeding ratios of Au^{3+} to peptides or the added NaOH amounts. The inset in Figure 1B is the lyophilized powder of AuNCs, showing that it can be scaled up. According to the inductively coupled plasma mass spectrometry (ICP-MS) determination results of Au^{3+} ions, the synthetic yield of pAuNCs from Au^{3+} ions is 45.8%.

Scheme 1. Molecular Structure of CCY−C6−CP Modular Peptide and the Illustration of Site-Specific Biomimetic Chemistry of pAuNCs via CCY−C6−CP[a]
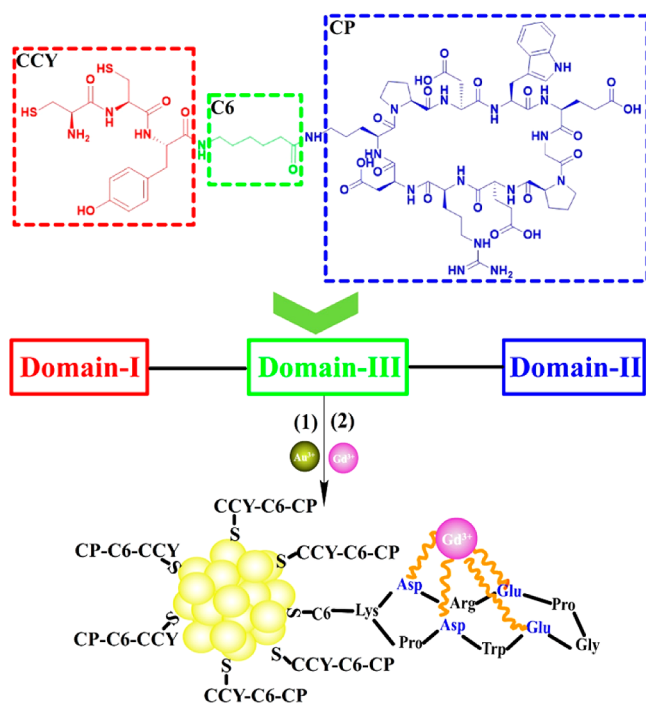
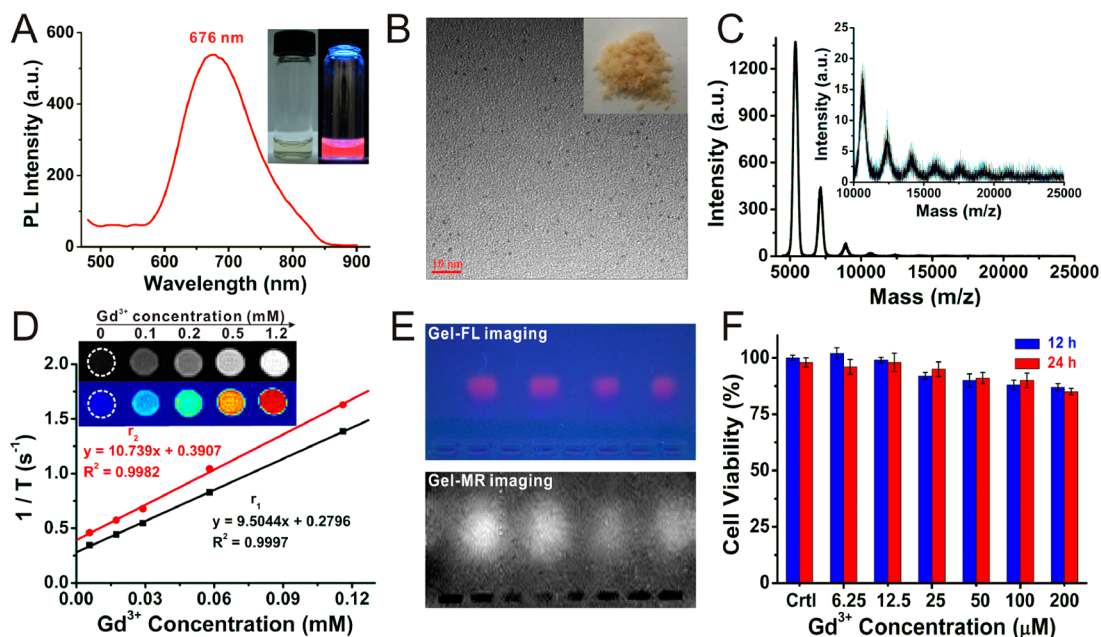[a]CP is the abbreviation of cyclic peptide.

Figure 1. Fluorescent emission spectrum of AuNCs; inset is the digital photos of prepared AuNCs under sunlight and a 365 nm lamp excitation (A). TEM image of AuNCs; inset is the lyophilized powder (B). Matrix-assisted laser desorption−ionization time of flight mass spectrometry spectrum of AuNCs; inset is the enlarged one for better revealing of the spectrum between 10 and ∼25 K m/z (C). From left to right, the peaks correspond to $Au_{25}S_{14}$, $Au_{25}S_{12}P$, $Au_{25}S_{10}P_2$, $Au_{25}S_8P_3$, $Au_{25}S_6P_4$, $Au_{25}S_4P_5$, and $Au_{25}S_2P_6$; herein, P is peptide. Relaxivity characterization and in vitro MR imaging of pAuNCs (D). Agarose gel electrophoresis of pAuNCs imaged by fluorescence and MR imaging (E). Cytotoxicity of the pAuNCs in Hela cells after 12 and 24 h of incubation (F).

The designed CCY−C6−CP modular peptide has been verified competent on biomimetic synthesis of fluorescent AuNCs. It is also primarily shown, as expected, that CCY motif plays a vital role in biosynthesis. To further investigate the site-specific biomimetic precision chemistry, MALDI-TOF MS was employed for its superior capability in identifying the accurate number of Au atoms and the peptides coating of AuNCs. The technique has been well-established for resolving quite a lot of AuNCs.[25,27,28] In this study, CCY−C6−CP@AuNCs was performed in a positive ion linear mode using sinapic acid (SA) as a matrix.

The MALDI-TOF MS spectrum of CCY−C6−CP@AuNCs is shown in Figure 1C. As can be seen in this figure, it is composed of a series of intense peaks between 5 and ∼25 K m/z. The inset is an enlarged one for the spectrum between 10 and ∼25 K m/z. The interval between adjacent maximum peak positions is very close to that of intact CCY−C6−CP (1692.9 Da). The m/z of the intense peaks basically matches the formula of $Au_{25}(CCY−C6−CP)_m S_{14−2m}$. Interestingly, it is accurate in the low-mass m/z range, while it becomes slightly deviated. In detail, the fractional errors for m values of 0−7 are 0.09%, 1.96%, 3.0%, 3.6%, 4.1%, 4.3%, 4.2% and 4.8%, respectively. These small variations were likely attributed to the small amount of impurity of the synthesized peptide. All intense peaks indicate a Au_{25} core capped by $(CCY−C6−CP)_m S_{14−2m}$ ($m = 0−7$). The sulfur atoms attached on the Au_{25} cluster originate from the cleaved C−S bond of cysteine in domain I of the peptide during the desorption−ionization laser processing.[25] As such, there is a strong negative correlation between the number of peptides attached to each Au cluster and the number of the attached sulfur atoms in the mass spectrum.

These results show the robust biomimetic synthesis of fluorescent Au_{25} nanoclusters with the designed peptide.

Fluorescent imaging shows good sensitivity to molecular information acquisition, and it becomes blurred in 3D structure illustration.[29] In this study, modular peptide was deliberately added with a unique amino acid sequence of CP for site-specific chelation of Gd^{3+} ions, aiming to provide MR structural imaging capability. Figure 1D shows that the Gd^{3+}-chelated AuNCs (termed by pAuNCs here) is paramagnetic with a higher relaxivity of r_1 (9.5 s^{-1} per mmol L^{-1} of Gd^{3+}) and r_2 (10.7 s^{-1} per mmol L^{-1} of Gd^{3+}) compared with that of commercially used Gd-DTPA (r_1 = 3.2 s^{-1} per mmol L^{-1} of Gd^{3+}, r_2 = 3.8 s^{-1} per mmol L^{-1} of Gd^{3+}). This improvement on relaxivity is mainly attributed to the suppression of molecular rotation.[30] The relatively low r_2/r_1 value of 1.13 favors pAuNCs as a T_1-weighted MR contrast agent. Further in vitro MR imaging of pAuNCs with varying Gd^{3+} concentrations from 0.1 to 1.2 mM plus pure water were performed, and the result is shown in the Figure 1D inset. By the use of T_1-weighted spin−echo sequences, it is found that the signal is gradually intensified with the increase of Gd^{3+} concentration. This enhancement pattern is consistent to the T_1 contrast characteristic of pAuNCs.

To demonstrate the integrity of pAuNCs, mediated by the modular peptide, the agarose gel electrophoresis technique was used for its superior capability in differentiating NPs with different sizes or surface ζ potentials.[31] pAuNCs were prepared for electrophoresis analysis with two different concentrations, and each has a duplicate. Under excitation with a 365 nm lamp, it shows that all four lanes have nearly the same band profile, which is narrow, bright, and without tailing area in the gel (Figure 1E). It suggests the structural uniformity and robust in fluorescence emission of the resultant pAuNCs. MR imaging followed, and the result shows highly co-localization of these two imaging patterns. Compared with the fluorescence imaging, the slight diffusion of pAuNCs in MR image is caused by the
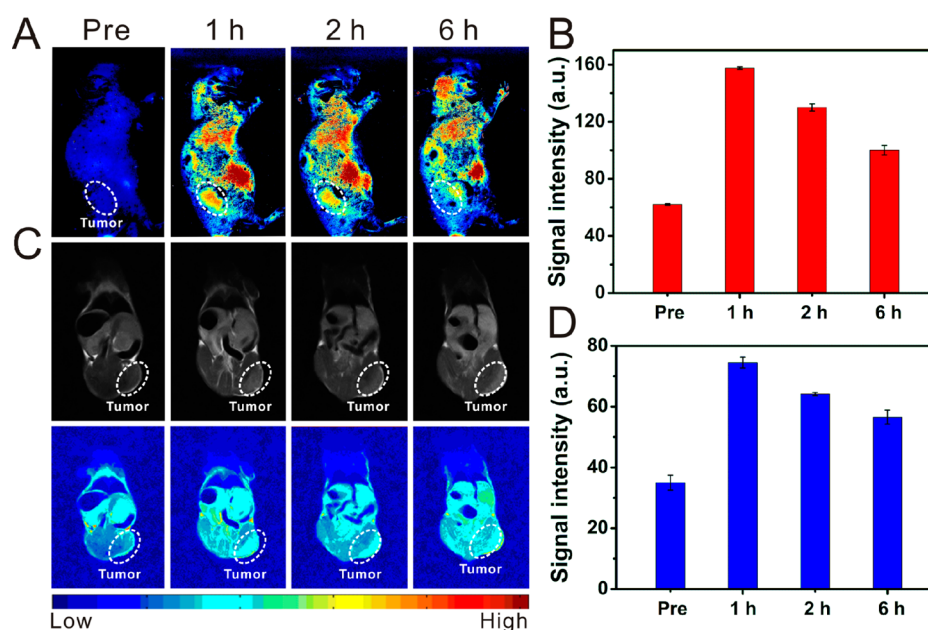
Figure 2. In vivo fluorescence (A) and MR imaging (C) of tumor-bearing nude mice taken before and after intravenous injection of pAuNCs at different time points, and the corresponding signal intensities at circled tumor area were quantified (B and D). The color scale bar is independently used for the signal strength comparison in the fluorescent or MR imaging.
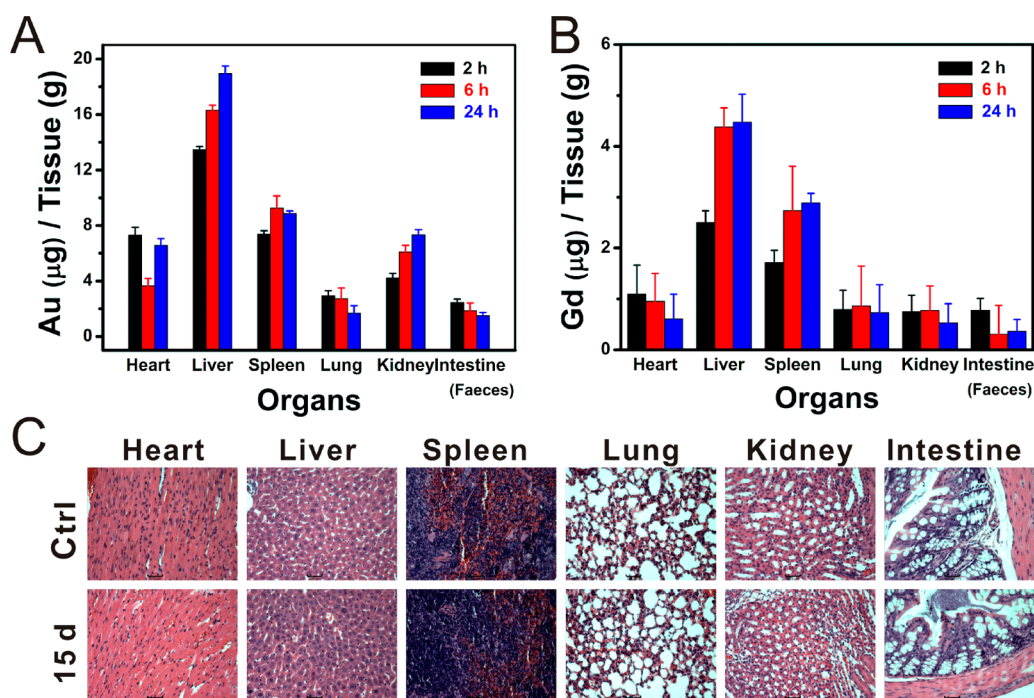

Figure 3. Biodistribution of pAuNCs assessed by Au (A) and Gd (B) elements at different time points in vivo. Hematoxylin and eosin stained pictures (200×) of major organs of mice, including the blank without administration and the ones after 15 days postinjection. Tissues were collected from hearts, livers, spleens, lungs, kidneys, and intestines.

delayed imaging scanning. The evidence on agarose gel electrophoresis analysis from another side demonstrates that the modular peptide with two separated domains can work independently on the biomimetic chemistry of bimodal pAuNCs. More importantly, it has demonstrated the possibility of the separated imaging moieties of pAuNCs. To further evaluate the stability of pAuNCs, pAuNCs were dialyzed against phosphate-buffered saline (PBS) buffer with 2% fetal bovine serum, and the dialysate was taken out every 2 h in 24 h

for ICP-MS determination of Gd^{3+} ions. Results shows that no Gd^{3+} was leaking, suggesting the successful conjuation of Gd chelates and AuNCs. The structural integrity of pAuNCs assisted by the modular peptide will resolutely enhance a single mode of pharmacokinetics in vivo.

Cytotoxicity of pAuNCs on Hela cells was evaluated. As can be seen in Figure 1F, after 12 and 24 h of incubation, more than 80% of Hela cells can survive at all concentrations, suggesting

enhanced biocompatibility by the biomimetic chemistry and raw materials employed in this work.

Figure 2A,C shows bimodal imaging of pAuNCs on tumor-bearing mice. The implemented tumors can be clearly enhanced in both fluorescent imaging and MR imaging after intravenous (i.v.) injection of pAuNCs. In particular, both imaging modalities show hyper-intensity achieves at 1 h post-injection, and the enhancement declines along with time. The corresponding intensities are further quantified as shown in Figure 2B,D. As expected, pAuNCs presents a univocal kinetics in vivo, corresponding to the in vitro co-localization of fluorescent imaging and MR imaging in agarose gel electrophoresis.

The detailed biodistribution of intravenously administrated pAuNCs in vivo is shown in Figure 3A,B. Dissolved Au^{3+} and Gd^{3+} ions from harvested organs have a similar distribution and tendency in the clearance process. Both indicate that pAuNCs experienced primary uptakes in liver and spleen and were gradually excluded from body via glomeruli and bile. In vivo bimodal imaging and biodistribution by intravenously injection collectively demonstrate good tumor targeting and strong stability in circulation of the modular peptide-bioinspired pAuNCs. In addition to the cytotoxicity test, the in vivo toxicity of pAuNCs was further investigated with hematoxylin and eosin (H&E) staining examination on the treated heart, liver, spleen, lung, kidney, and intestine tissues. Compared with the control group, there is no notable histological change of the involved tissues after exposure to pAuNCs (Figure 3C). All of the mice were found without any weight loss, illness, or abnormal behaviors during the investigated period. Evidence from in vitro cytotoxicity and in vivo histological studies suggest that pAuNCs are slightly toxic.

In conclusion, the designed modular peptide enables the in situ site-specific precision synthesis of paramagnetic and fluorescent ultrafine gold nanoclusters. This biomimetic strategy is found to be effective, straightforward, and environmentally benign. The bioinspired pAuNCs show good stability, excellent biocompatibility, and high relaxivity. In vivo bimodal imaging reveals potent tumor selective enhancement by pAuNCs in mice. No obvious toxicity is found in the in vitro or in vivo toxicity tests. Biodistribution suggests pAuNCs can be dispelled from body in a hepatic and renal hybrid pattern.

By the combination of selected elements, biomimetic chemistry is shown to demonstrate a generalized strategy for chemoselective engineering of modular peptide, which site-specifically incubates bimodal NPs with high efficacy and facilitates efficient delivery to the tumors. The amino acids or amino acid sequences, which are conjectured with the capability of biomimetic chemistry, can be spliced into short peptides and used to verify the hypothesis. Based on this concept, other proteins or peptides can be found and used in biomimetic synthesis for cancer nanotheranostics.

ASSOCIATED CONTENT

Ⓢ Supporting Information

The Supporting Information is available free of charge on the ACS Publications website at DOI: 10.1021/acs.bioconjchem.6b00712.

> Experimental details, mass and absorption spectra, images showing the effects of Au^{3+} ions and NaOH on fluorescence emission, and a size distribution histogram. (PDF)

AUTHOR INFORMATION

Corresponding Authors
*E-mail: drfxm@163.com.
*E-mail: shid@ucmail.uc.edu.

ORCID Ⓞ
Bingbo Zhang: 0000-0002-0981-7071

Notes
The authors declare no competing financial interest.

REFERENCES

(1) Kievit, F. M., and Zhang, M. (2011) Cancer nanotheranostics: improving imaging and therapy by targeted delivery across biological barriers. *Adv. Mater. 23*, H217−H247.

(2) Tian, J., Chen, J., Ge, C., Liu, X., He, J., Ni, P., and Pan, Y. (2016) Synthesis of PEGylated Ferrocene Nanoconjugates as the Radio-sensitizer of Cancer Cells. *Bioconjugate Chem. 27*, 1518−1524.

(3) Guo, W., Yang, W., Wang, Y., Sun, X., Liu, Z., Zhang, B., Chang, J., and Chen, X. (2014) Color-tunable Gd-Zn-Cu-In-S/ZnS quantum dots for dual modality magnetic resonance and fluorescence imaging. *Nano Res. 7*, 1581−1591.

(4) Wu, X., Chen, G., Shen, J., Li, Z., Zhang, Y., and Han, G. (2015) Upconversion nanoparticles: a versatile solution to multiscale biological imaging. *Bioconjugate Chem. 26*, 166−175.

(5) Xiong, L., Shen, B., Behera, D., Gambhir, S. S., Chin, F. T., and Rao, J. (2013) Synthesis of ligand-functionalized water-soluble [18 F] YF 3 nanoparticles for PET imaging. *Nanoscale 5*, 3253−3256.

(6) Mauriello-Jimenez, C., Croissant, J., Maynadier, M., Cattoën, X., Man, M. W. C., Vergnaud, J., Chaleix, V., Sol, V., Garcia, M., Gary-Bobo, M., et al. (2015) Porphyrin-functionalized mesoporous organosilica nanoparticles for two-photon imaging of cancer cells and drug delivery. *J. Mater. Chem. B 3*, 3681−3684.

(7) Wang, Y., Ji, L., Zhang, B., Yin, P., Qiu, Y., Song, D., Zhou, J., and Li, Q. (2013) Upconverting rare-earth nanoparticles with a para-magnetic lanthanide complex shell for upconversion fluorescent and magnetic resonance dual-modality imaging. *Nanotechnology 24*, 175101.

(8) Tilley, R. D., Warner, J. H., Yamamoto, K., Matsui, I., and Fujimori, H. (2005) Micro-emulsion synthesis of monodisperse surface stabilized silicon nanocrystals. *Chem. Commun. 14*, 1833−1835.

(9) Hufschmid, R., Arami, H., Ferguson, R. M., Gonzales, M., Teeman, E., Brush, L. N., Browning, N. D., and Krishnan, K. M. (2015) Synthesis of phase-pure and monodisperse iron oxide nanoparticles by thermal decomposition. *Nanoscale 7*, 11142−11154.

(10) Ling, D., Lee, N., and Hyeon, T. (2015) Chemical synthesis and assembly of uniformly sized iron oxide nanoparticles for medical applications. *Acc. Chem. Res. 48*, 1276−1285.

(11) Ni, D., Bu, W., Zhang, S., Zheng, X., Li, M., Xing, H., Xiao, Q., Liu, Y., Hua, Y., Zhou, L., et al. (2014) Single Ho3+ -Doped Upconversion Nanoparticles for High -Performance T2-Weighted Brain Tumor Diagnosis and MR/UCL/CT Multimodal Imaging. *Adv. Funct. Mater. 24*, 6613−6620.

(12) Hoffman, A. S. (2013) Stimuli-responsive polymers: Biomedical applications and challenges for clinical translation. *Adv. Drug Delivery Rev. 65*, 10−16.

(13) Shi, J., Kantoff, P. W., Wooster, R., and Farokhzad, O. C. (2016) Cancer nanomedicine: progress, challenges and opportunities. *Nat. Rev. Cancer 17*, 20−37.

(14) Wilhelm, S., Tavares, A. J., Dai, Q., Ohta, S., Audet, J., Dvorak, H. F., and Chan, W. C. (2016) Analysis of nanoparticle delivery to tumours. *Nat. Rev. Mater. 1*, 16014.

(15) Yang, W., Guo, W., Chang, J., and Zhang, B. (2017) Protein/peptide-templated biomimetic synthesis of inorganic nanoparticles for biomedical applications. *J. Mater. Chem. B*, DOI: 10.1039/C6TB02308H.

(16) Zhang, B., Wang, X., Liu, F., Cheng, Y., and Shi, D. (2012) Effective reduction of nonspecific binding by surface engineering of quantum dots with bovine serum albumin for cell-targeted imaging. *Langmuir 28*, 16605−16613.

(17) Zhang, J., Hao, G., Yao, C., Hu, S., Hu, C., and Zhang, B. (2016) Paramagnetic albumin decorated CuInS 2/ZnS QDs for CD133+ glioma bimodal MR/fluorescence targeted imaging. *J. Mater. Chem. B 4*, 4110−4118.

(18) Wang, X., Xing, X., Zhang, B., Liu, F., Cheng, Y., and Shi, D. (2014) Surface engineered antifouling optomagnetic SPIONs for bimodal targeted imaging of pancreatic cancer cells. *Int. J. Nanomed. 9*, 1601−1615.

(19) Du, H., Yu, J., Guo, D., Yang, W., Wang, J., and Zhang, B. (2016) Improving the MR Imaging Sensitivity of Upconversion Nanoparticles by an Internal and External Incorporation of the Gd3+ Strategy for in Vivo Tumor-Targeted Imaging. *Langmuir 32*, 1155−1165.

(20) Zhang, A., Tu, Y., Qin, S., Li, Y., Zhou, J., Chen, N., Lu, Q., and Zhang, B. (2012) Gold nanoclusters as contrast agents for fluorescent and X-ray dual-modality imaging. *J. Colloid Interface Sci. 372*, 239−244.

(21) Xie, J., Zheng, Y., and Ying, J. Y. (2009) Protein-directed synthesis of highly fluorescent gold nanoclusters. *J. Am. Chem. Soc. 131*, 888−889.

(22) Yang, W., Guo, W., Le, W., Lv, G., Zhang, F., Shi, L., Wang, X., Wang, J., Wang, S., Chang, J., and Zhang, B. (2016) Albumin-Bioinspired Gd: CuS Nanotheranostic Agent for In Vivo Photoacoustic/Magnetic Resonance Imaging-Guided Tumor-Targeted Photothermal Therapy. *ACS Nano 10*, 10245−10257.

(23) Weitao, Y., Weisheng, G., Bingbo, Z., and Jin, C. (2014) Synthesis of Noble Metal Nanoclusters Based on Protein and Peptide as a Template. *Huaxue Xuebao 72*, 1209−1217.

(24) Le Guével, X., Hötzer, B., Jung, G., Hollemeyer, K., Trouillet, V., and Schneider, M. (2011) Formation of fluorescent metal (Au, Ag) nanoclusters capped in bovine serum albumin followed by fluorescence and spectroscopy. *J. Phys. Chem. C 115*, 10955−10963.

(25) Wang, Y., Cui, Y., Zhao, Y., Liu, R., Sun, Z., Li, W., and Gao, X. (2012) Bifunctional peptides that precisely biomineralize Au clusters and specifically stain cell nuclei. *Chem. Commun. 48*, 871−873.

(26) Xie, J., Lee, J. Y., Wang, D. I., and Ting, Y. P. (2007) Silver nanoplates: from biological to biomimetic synthesis. *ACS Nano 1*, 429−439.

(27) Cui, Y., Wang, Y., Liu, R., Sun, Z., Wei, Y., Zhao, Y., and Gao, X. (2011) Serial silver clusters biomineralized by one peptide. *ACS Nano 5*, 8684−8689.

(28) Dass, A., Stevenson, A., Dubay, G. R., Tracy, J. B., and Murray, R. W. (2008) Nanoparticle MALDI-TOF mass spectrometry without fragmentation: Au25 (SCH2CH2Ph) 18 and mixed monolayer Au25 (SCH2CH2Ph) 18− x (L) x. *J. Am. Chem. Soc. 130*, 5940−5946.

(29) Lv, R., Yang, P., He, F., Gai, S., Li, C., Dai, Y., Yang, G., and Lin, J. (2015) A yolk-like multifunctional platform for multimodal imaging and synergistic therapy triggered by a single near-infrared light. *ACS Nano 9*, 1630−1647.

(30) Zhang, Z., Greenfield, M. T., Spiller, M., McMurry, T. J., Lauffer, R. B., and Caravan, P. (2005) Multilocus Binding Increases the Relaxivity of Protein-Bound MRI Contrast Agents. *Angew. Chem., Int. Ed. 44*, 6766−6769.

(31) Zhang, B., Xing, D., Lin, C., Guo, F., Zhao, P., Wen, X., Bao, Z., and Shi, D. (2011) Improving colloidal properties of quantum dots with combined silica and polymer coatings for in vitro immuofluorenscence assay. *J. Nanopart. Res. 13*, 2407−2415.